

Crystal Structure of a Modulated Composite Structure with Two Subsystems: $\text{Ba}_{1.1064}\text{CoO}_3$

A. El Abed,^{*,†} S. E. Elqebbaj,[†] M. Zakhour,^{*} M. Champeaux,^{*}
J. M. Perez-Mato,[‡] and J. Darriet^{*,1}

^{*}Institut de Chimie de la Matière Condensée de Bordeaux (ICMCB-CNRS), 87 Av. du docteur A. Schweitzer, 33608 Pessac cedex, France; [†]Laboratoire de Physique du Solide, Faculté des Sciences, Université Mohamed I, Oujda, Maroc; and [‡]Departamento de Física de la Materia Condensada, Facultad de Ciencias, Universidad del País Vasco, Apdo 644, 48080 Bilbao, Spain

Received May 2, 2001; in revised form July 10, 2001; accepted July 12, 2001

The structure of $\text{Ba}_{1.1064}\text{CoO}_3$ has been solved in the (3 + 1)-dimensional formalism. The structure is described as a modulated chain composite with two subsystems, $[\text{CoO}_3]$ and $[\text{Ba}]$, respectively. The superspace group is $R\text{-}3m(00\gamma)0s$ with $a = 9.8842(20)\text{Å}$, $c = 2.4785(12)\text{Å}$, and $q = 0.5532(4)$ c^* ($Z = 3$). A saw-tooth function was used to model both the occupational and displacive modulations. Each atomic saw-tooth function is defined by its center \hat{x}_4 along the fourth dimension, its width (Δ), and the maximum amplitude of the displacive modulation (δ). The paper describes how, as a first approximation, the columns (CoO_3) can be mainly described by a single free parameter, based on the height difference of the trigonal prisms and octahedra that constitute the transition metal chains. As a result, this superspace formalism requires only a small number of variables to be refined, compared to the conventional superstructure description. © 2001 Academic Press

Key Words: barium cobalt oxide; superspace formalism; modulated composite structure.

INTRODUCTION

An hexagonal perovskite family of the general formula $A_{1+x}(A'_xB_{1-x})\text{O}_3$ ($A = \text{Ca}, \text{Sr}, \text{Ba}, \text{etc.}$ and $A', B = d$ transition metal) have recently been reported (1–11). The main feature of these compounds is that their structure is made of one-dimensional chains of transition metal built up of octahedra and trigonal prisms sharing faces which can possess unusual electronic properties, the chains being separated by columns of A cations. It has been recognized that these structures are strongly related to the 2H hexagonal perovskite (1). The crystal structures can be described as stacking of mixed $[\text{A}_3\text{O}_9]$ and $[\text{A}_3\text{A}'\text{O}_6]$ layers with B^{IV} elements occupying the octahedral sites between these layers

¹To whom correspondence should be addressed. E-mail: darriet@icmcb.u-bordeaux.fr.

and the A^{II} cations filling trigonal prismatic sites (1,2). Although such an ideal layer model is useful for predicting the compositions of different members of the family (1–11), no general unique rule for the sequence of octahedra and trigonal prisms within the chains can be predicted. Moreover, the ideal layer model considers that the geometry of the octahedral and prismatic units along the chains is rigid with the condition $D_p = 2D_o$, where D_p is the height of the trigonal prism and D_o is the height of the octahedron. The model also requires that the A atoms are located either at the z level of the center of a triangular prism ($\text{A}_3\text{A}'\text{O}_6$ layer) or at the level of the oxygen (A_3O_9 layer).

A more unifying picture of the family is obtained if the compounds are described as modulated composite structures with two chain subsystems: an $[\text{A}'_xB_{1-x}\text{O}_3]$ first chain subsystem with a varying succession of face sharing $[\text{B}^{\text{IV}}\text{O}_6]$ octahedra and $[\text{A}^{\text{II}}\text{O}_6]$ trigonal prisms, and an $[\text{A}]$ second chain subsystem (12–18).

Detailed explanation of the composite structure approach and its description using the superspace formalism can be found in (19–23) and references therein. The whole family can be simply described within the frame of a unique general model. All the structures have the same (3 + 1) dimensional superspace group. Then, long-period superstructure can be easily refined within that model which otherwise could be very difficult with a conventional three-dimensional approach.

Precise structure determinations using the superspace formalism have shown the unity of the series and evidenced some peculiar characteristics, such as the instability of M^{II} ions in their trigonal prismatic sites, with a displacement of the cations out of the site center (13, 14, 16–18).

Different members of the $\text{Ba}_{1+x}\text{CoO}_3$ homologues series have been observed by electron diffraction microscopy (9–11).

The aim of the present paper is to show, through the structure of a member of this series, the efficiency of the 4-dimensional superspace formalism.



EXPERIMENTAL

Synthesis

The single crystal selected for structure determination was prepared by flux synthesis using a method described previously (24). A total of 1 g of BaCO₃ (99.99% purity) and Co₃O₄ (99.9986% purity) corresponding to the global composition Ba_{1.0/9}CoO₃ was ground for 15 min and placed into an alumina crucible. Twenty grams of K₂CO₃ was packed into the crucible on top of the reagents. The crucible was covered with alumina disc to minimize the flux evaporation. The sample was heated in air from room temperature to the reaction temperature (950°C) at 60°C/h. The crucible was held at this temperature for 3 days and cooled at 6°C/h to 880°C. The furnace was then turned off and the system was cooled down to room temperature. The crystals were washed with distilled water and dried. Well defined black metallic needles free of K could then be isolated.

Data Collection

Prior to data collection, the selected crystal was carefully checked for quality using Weissenberg and precession cameras. In both cases, it was determined that the single crystal is twinned with a transformation matrix (−100/0 −100/001). These film studies show that the structures are in fact misfit composite crystal with two trigonal/hexagonal subsystems with common *a* and *b* axes but different *c* axes: *a* ≈ 9.88 Å, *c*₁ ≈ 2.48 Å, *c*₂ ≈ 4.48 Å. The first one related to the [CoO₃] part is rhombohedral with *c*₁ ≈ 2.48 Å while the second related to the [Ba] part is hexagonal with *c*₂ ≈ 4.48 Å. The *a* and *b* axes are common. Both structures are modulated along *z* with a modulation period given by the average *c* parameter of the other subsystem; i.e., the modulation wave-vector of subsystem [CoO₃] is *c*₂^{*} and vice versa. The two subsystems can be analyzed separately as two independent modulated structures in direct space. However, their diffraction pattern superpose coherently in reciprocal space and then each Bragg reflection *H* is expressed as *H* = *ha*^{*} + *kb*^{*} + *lc*₁^{*} + *mc*₂^{*}. The so-called “main” reflections (*h, k, l, 0*) with *l* ≠ 0 and (*h, k, 0, m*) with *m* ≠ 0 are interpreted as the Bragg reflections of the subsystems 1 and 2, respectively, if the modulations are neglected. In that case, “authentic” satellite reflections (*h, k, l, m*) with both *l* and *m* ≠ 0 could not exist. The modulation of both systems, however, generates these satellites plus nonnegligible contributions of both subsystems to the two sets of main reflections.

As explained in (13–15), a precise determination of the ratio $\gamma = c_2^*/c_1^* = c_1/c_2$ between the reciprocal parameters *c*₁^{*} and *c*₂^{*} is sufficient for deriving the compound composition through the relation $\gamma = (1 + x)/2$.

The data collection was carried out in successive steps. Initially, the *c*₁ and *c*₂ parameters were determined. For

each subsystem 25 reflections were centered and then additional reflections were measured at higher θ -values in order to get precise values of the cell parameters. The refinement led to the following lattice parameters: *a* = 9.8842(20) Å, *c*₁ = 2.4785(12) Å for [CoO₃] subsystem and *a* = 9.8842(20) Å, *c*₂ = 4.4805 (14) Å for [Ba] subsystem. If the [CoO₃] subsystem is chosen as the reference, the *q* vector is $q = \gamma c_1^* = 0.5532(4)c_1^*$, hence $x = 0.1064$. The experimental γ value is relatively close to the $\frac{5}{9}$ (0.5556) rational ratio (difference < 6σ(γ)), which would correspond to $x = \frac{1}{9}$. Therefore, the structure has been refined both in the incommensurate and commensurate models for comparison.

Intensity data were collected in the supercell approach corresponding to $\gamma = \frac{5}{9}$. The transformation of the 3D indices to (3 + 1)D *hkml* values was performed using the JANA98 program package (25).

The [CoO₃] subsystem was chosen as the reference system. The two possible superspace groups that are compatible with the observed extinction conditions of $-h + k + l \neq 3n$ for *hkml* and $m \neq 2n$ for *h0lm* are *R*3*m*(00 γ)0*s* and *R* $\bar{3}$ *m*(00 γ)0*s*.

TABLE 1
Cristallographic Data for Ba_{1+x}CoO₃ with *x* = 0.1064

Formula	Ba _{1.1064} CoO ₃
Crystal color	Black
MW (g mole ⁻¹)	258.8
Superspace group	<i>R</i> $\bar{3}$ <i>m</i> (00 γ)0 <i>s</i>
Parameters	<i>a</i> = 9.8842(20) Å, <i>c</i> ₁ = 2.4785(12) Å, <i>q</i> = 0.5532 (2) <i>c</i> ₁ [*]
<i>V</i> (Å ³)	209.7 (1)
<i>Z</i>	3
Density calculation (g cm ⁻³)	6.15
Crystal description	Needle
Crystal dimensions	0.21 × 0.025 × 0.02 mm
Monochromator	Oriented graphite
Radiation	MoK α (λ = 0.71073 Å)
Scan mode	$\omega/2\theta$
<i>hkl</i> range	0 < <i>h</i> < 16 −16 < <i>k</i> < 16 −37 < <i>l</i> < 0
θ_{\max}	40°
Absorption correction	Psi Scan
<i>T</i> _{min} / <i>T</i> _{max}	0.77/1
Number of measured reflections	10201
Number observed reflections	3849
Number independent reflections	1306 <i>I</i> > 3σ(<i>I</i>) <i>R</i> _{int} = 4.89%
Twin matrix	$\bar{1}00/0\bar{1}0/001$
% twin	34.9 (1)%
<i>F</i> (000)	339
<i>R</i> factors (on <i>F</i>) [*]	<i>R</i> = 4.06% <i>R</i> _w = 4.20%
Main reflections (326)	<i>R</i> = 2.55% <i>R</i> _w = 3.03%
First order (655)	<i>R</i> = 4.92% <i>R</i> _w = 4.68%
Second order (325)	<i>R</i> = 8.09% <i>R</i> _w = 7.62%
Number refined parameters	43
Diff. Fourier residues (e ⁻ /Å ³)	(−4.6, +3.6)

$$*R = \frac{\sum \|F_o\| - \|F_c\|}{\sum \|F_o\| R_w} = \frac{[\sum w(\|F_o\| - \|F_c\|)^2 / \sum w \|F_o\|^2]^{1/2}}{w = 1/(\sigma^2 \|F_o\|)}$$

TABLE 2
Average Atomic Positions

Atoms	x_0	y_0	z_0	$U_{\text{eq}}^* (\text{\AA}^2) \times 10^4$
Subsystem [CoO ₃]: $R\bar{3}m(00\gamma)0s$				
Co ₁	0	0	0	92(1)
Co ₂	0	0	0	340(10)
O	0.1486(1)	0.1486(1)	$\frac{1}{2}$	147(4)
Subsystem [Ba]: $P\bar{3}c1(001/\gamma)$				
Atoms	x_0	y_0	z_0	$U_{\text{eq}}^* (\text{\AA}^2) \times 10^4$
Ba ₁	0.3249(2)	0	$\frac{1}{4}$	131(5)
Ba ₂	0.3488(5)	0	$\frac{1}{4}$	54(4)

$$U_{\text{eq}} = \frac{1}{3} \sum_i \sum_j U^{ij} a_i^* a_j^* \mathbf{a}_i \cdot \mathbf{a}_j$$

Measured intensities were corrected for decay on the basis of three standard reflections, as well as for Lorentz and polarization effects. Absorption corrections were applied using the Ψ -scan technique. Crystal data and details of the data collection are given in Table 1.

RESULTS AND DISCUSSION

Following the theoretical description of the structure of the $A_{1+x}(A'_x B_{1-x})O_3$ series (13–15), the centrosymmetric $R\bar{3}m(00\gamma)0s$ superspace group was chosen since it allows the generation of the atomic position of the oxygen atoms needed to create the octahedra and trigonal prisms.

Incommensurate Option

[CoO₃] subsystem. As mentioned before, the [CoO₃] subsystem was chosen as the reference. The corresponding superspace group is $R\bar{3}m(00\gamma)0s$ ($Z = 3$) and the space group of the average structure is $R\bar{3}m$. As proposed in Ref. (15), a saw-tooth type function defined by its center (\hat{x}_4), its width (Δ) along the x_4 internal axis, and a maximum amplitude for the displacive z component was used to account for the atoms. The average cobalt atomic position was (000). Two cobalt saw-tooth functions were considered, they were associated to the trigonal prisms and the octahedra in [CoO₃] chains along the z axis. The first function, centered

TABLE 3
Average Anisotropic Displacement Parameters $U^{ij} (\text{\AA})^2$
for Ba_{1.1064}CoO₃

	U^{11}	U^{22}	U^{33}	U^{12}	U^{13}	U^{23}
Co ₁	0.0069(1)	$= U^{11}$	0.0138(2)	$= \frac{1}{2} U^{11}$	0	0
Co ₂	0.0067(6)	$= U^{11}$	0.090(3)	$= \frac{1}{2} U^{11}$	0	0
O	0.0099(3)	$= U^{11}$	0.0206(7)	0.0021(4)	0.0002(3)	$= -U^{13}$
Ba ₁	0.0058(9)	0.0189(4)	0.0190(4)	$= \frac{1}{2} U^{22}$	0.00506(7)	$= 2U^{13}$
Ba ₂	0.0039(5)	0.0017(6)	0.0099(6)	$= \frac{1}{2} U^{22}$	0.0002(2)	$= 2U^{13}$

TABLE 4
Atomic Positional and Displacement Factors and Modulation Coefficients for Ba_{1.1064}CoO₃ (Only Coefficients $\neq 0$ are Given)

Co ₁	$U_{z,1}^{\text{Co}_1} = -0.0235(2)$		
	Amplitude = $-0.8936\delta_{\text{O}}/c_1$	$\hat{x}_4 = 0$	$\Delta = 0.4468$
	$U_{U^{11,2}}^{\text{Co}_1} = U_{U^{23,2}}^{\text{Co}_1} = 2U_{U^{12,2}}^{\text{Co}_1}$		
	$= -0.0031(1)$		
	$U_{U^{33,2}}^{\text{Co}_1} = -0.0036(3)$		
Co ₂	Amplitude = $-0.1064\delta_{\text{O}}/c_1$	$\hat{x}_4 = \frac{1}{4}$	$\Delta = 0.0532$
O	$U_{x,1}^{\text{O}} = U_{y,1}^{\text{O}} = 0.0016(1)$		
	$U_{x,2}^{\text{O}} = -U_{y,2}^{\text{O}} = -0.00075(8)$	$U_{z,2}^{\text{O}} = 0.0338(7)$	
	Amplitude = $-0.11134 = -\delta_{\text{O}}/c_1$	$\hat{x}_4 = \frac{1}{4}$	$\Delta = \frac{1}{2}$
	$U_{U^{11,1}}^{\text{O}} = U_{U^{22,1}}^{\text{O}} = -0.0054(4)$	$U_{U^{33,1}}^{\text{O}} = -0.0095(9)$	
	$U_{U^{12,1}}^{\text{O}} = -0.0011(5)$	$U_{U^{13,1}}^{\text{O}} = -U_{U^{23,1}}^{\text{O}}$	$= -0.0004(4)$
	$U_{U^{11,2}}^{\text{O}} = -U_{U^{22,2}}^{\text{O}} = -0.00003(40)$		
	$U_{U^{13,2}}^{\text{O}} = U_{U^{23,2}}^{\text{O}} = 0.0020(4)$		
Ba ₁	$\hat{x}_4 = \frac{1}{2}$	$\Delta = 0.237166$	
	$2U_{x,1}^{\text{Ba}_1} = U_{y,1}^{\text{Ba}_1} = -0.0061(3)$	$U_{z,1}^{\text{Ba}_1} = 0.0015(3)$	
	$U_{x,2}^{\text{Ba}_1} = 0.0096(7)$		
	$U_{U^{11,1}}^{\text{Ba}_1} = U_{U^{12,1}}^{\text{Ba}_1} = 0.0004(4)$	$U_{U^{13,1}}^{\text{Ba}_1} = -0.0008(3)$	
	$U_{U^{11,2}}^{\text{Ba}_1} = 0.0005(5)$	$U_{U^{23,2}}^{\text{Ba}_1} = 2U_{U^{13,2}}^{\text{Ba}_1} = -0.0015(7)$	
	$U_{U^{33,2}}^{\text{Ba}_1} = 0.0031(5)$	$U_{U^{23,2}}^{\text{Ba}_1} = 2U_{U^{13,2}}^{\text{Ba}_1} = -0.0001(3)$	
Ba ₂	$\hat{x}_4 = 0$	$\Delta = 0.096168$	

* Modulation functions for a parameter λ of an atom v defined in a restricted interval are given by: $U_{\lambda,n}^v(x_4) = \sum_{n=0}^k U_{\lambda,n}^v \text{Ortho}_n^v(x_4)$, where the orthogonalized functions, obtained through a Schmidt orthogonalization routine, are given by: $\text{Ortho}_n^v(x_4) = B_0^v + \sum_{n=1}^k A_n^v \sin(2\pi n x_4) + \sum_{n=1}^k B_n^v \cos(2\pi n x_4)$ with coefficients B_0^v , A_n^v , and B_n^v given in Table 5.

at $\hat{x}_4 = 0$ with a width of 0.44680 ($\Delta = (1-x)/2$) corresponds to the cobalt atom in the octahedra while the second function centered at $\hat{x}_4 = \frac{1}{4}$ with a width of 0.05320 ($\Delta = x/2$) describes the cobalt in the trigonal prisms.

The average position of the oxygen atoms is $(x, x, \frac{1}{2})$ ($x \approx \frac{1}{6}$) and by the ternary axis six positions are generated in the same plane $z = \frac{1}{2}$. These six average positions can be separated into two types, O_a and O_b, forming two equilateral triangles, which correspond to the two possible orientations of the triangular O₃ faces in the [CoO₃] chains (13, 15). The average oxygen at $(x, x, \frac{1}{2})$ (type O_a) is invariant for the binary axis 2_{xy} . According to the superspace group, this binary axis is associated to a translation $\frac{1}{2}$ along x_4 . If $pO_a(x_4)$ stands for the occupancy of O_a, then $pO_a(x_4) = pO_a(-x_4 + \frac{1}{2})$ and $pO_b(x_4) = pO_a(x_4 - \frac{1}{2})$ (the O_b atoms are translated by $\frac{1}{2}$ along x_4). Under the assumption that the two types of sites are either fully occupied or empty, the simplest atomic modulation function $pO_a(x_4)$ compatible with the symmetry condition is a Crenel function (26, 27) with a width $\Delta = \frac{1}{2}$, centered at $x_4 = \frac{1}{4}$. Depending on the value of the Crenel function along x_4 , either set O_a or set O_b is fully occupied along the real z axis. Two

TABLE 5
Coefficients of the Orthogonalized Functions

Ortho _i ^O	B ₀ ^O	A ₁ ^O	B ₁ ^O
Ortho ₀ ^O	1		
Ortho ₁ ^O	-2.069	3.249	
Ortho ₂ ^O	0	0	1.414
Ortho _i ^{Co1}	B ₀ ^{Co1}	A ₁ ^{Co1}	B ₁ ^{Co1}
Ortho ₀ ^{Co1}	1		
Ortho ₁ ^{Co1}	0	1.505	
Ortho ₂ ^{Co1}	-2.757	0	3.924
Ortho _i ^{Ba1}	B ₀ ^{Ba1}	A ₁ ^{Ba1}	B ₂ ^{Ba1}
Ortho ₀ ^{Ba1}	1		
Ortho ₁ ^{Ba1}	0	2.458	
Ortho ₂ ^{Ba1}	-2.372	0	3.546

adjacent O_a-O_a or O_b-O_b triangles create a trigonal prism.

The oxygen positions must have some z displacement in order to distinguish the two types of sites. The simplest hypothesis is to consider that all prisms have the same length D_p along z and the octahedra the same length D_o . This can be achieved by considering a saw-tooth modulation for the displacive AMFs of the oxygens. The maximum amplitude of the displacive AMFs is the single free parameter $\delta_o = (D_p - D_o)/2$ (15).

If the cobalt sites (A' and B) are assumed to be in the median plane of the trigonal prisms (A' site) and the octahedra (B site), the maximum amplitudes of the displacive AMFs of the cobalt are related to δ_o by the relations $\delta_{A'} = x\delta_o$ and $\delta_B = (1 - x)\delta_o$, respectively (15-18).

[Ba] subsystem. The superspace group of the [Ba] subsystem is $P\bar{3}c1(001/\gamma)$. Two positions for the barium are considered whether they belong to the [Ba₃O₉] layer (Ba₁) or to the [Ba₃CoO₆] layer (Ba₂). The average positions are $(x0\frac{1}{4})$ ($x = \frac{1}{3}$). For Ba₁, the Crenel function is centered in $\hat{x}_4 = \frac{1}{2}$ with a width of $\Delta = 0.23717$ ($\Delta = (1 - 2x)/3(1 + x)$) and for Ba₂ $\hat{x}_4 = 0$, $\Delta = 0.09617$ ($\Delta = x/(1 + x)$) (15).

The first stage of the refinement was carried out considering the δ_o value as the only refinable parameters for the AMFs for the [CoO₃] subsystem. Modulations in the plane xy allowed by symmetry were kept to zero. For the [Ba] subsystem no modulations were considered. The residual factor R was 12.1%. Then after successive steps, the anisotropic displacement factors of all the atoms and the second order displacive Fourier amplitude waves for Co₁ (octahedral site) and the oxygen were introduced in the refinement. The residual factor R decreases to 5.9%. These second order displacive AMFs introduce modulations in the plane xy for

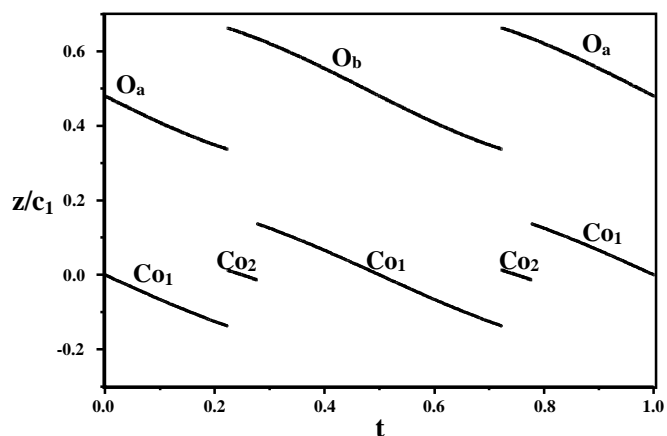


FIG. 1. Graphical representation of the fractional z coordinate of [CoO₃] subsystem versus the internal coordinate t ($t = x_4 - q.r_{av}$)

the considered atoms. To avoid correlations, the amplitudes refer to a basis of functions of period 1 along the internal coordinate x_4 , but orthogonalized within the Δ interval associated to the corresponding occupational Crenel function (26).

The JANA 98 program package has been kindly adapted to the saw-tooth functions by its authors (Petricek *et al.*).

In a final step, the displacive modulations of Ba₁ described by a Fourier series and the first order Fourier amplitudes for the atomic displacement parameters for Co₁, O, and Ba₁ were included in the refinement. Then the final residual factor R was stabilized at 4.06% for 43 independent refined parameters (Table 1). The final parameters are gathered in Tables 2-5.

Commensurate option. As written previously, the experimental q value (0.5532) is not so far from the simple rational value $\frac{5}{9}$ (0.5555...) and therefore a refinement was carried out in the commensurate option. For $\gamma = p/k$ with both

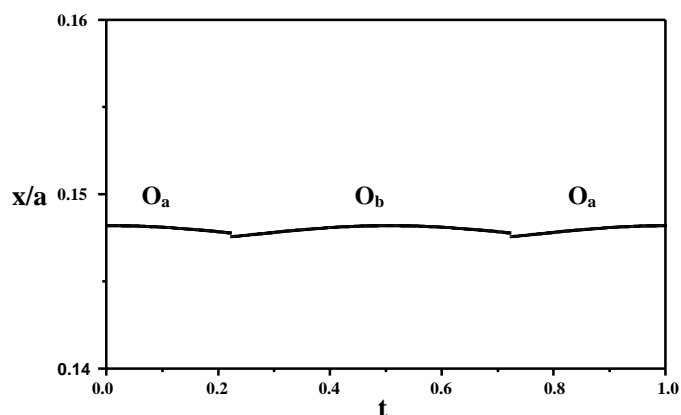


FIG. 2. Graphical representation of the fractional x ($= y$) coordinate for O_a and O_b versus the internal coordinate t .

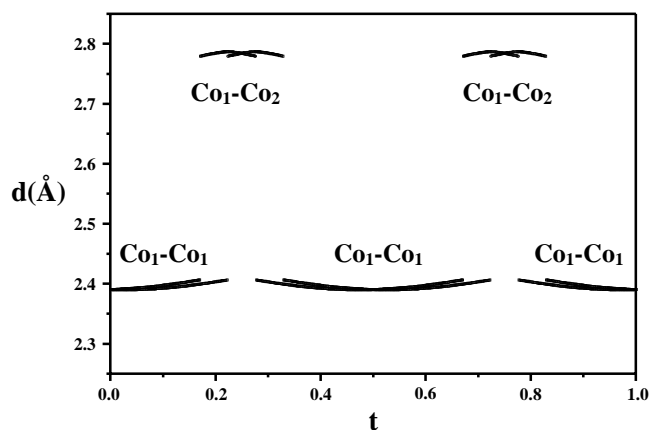


FIG. 3. Co-Co distances versus t for $\text{Ba}_{1.1064}\text{CoO}_3$.

p and k odd and $p \neq 3n$, three possible three-dimensional space-groups ($P-3$, $P32$, and $P3$) are deduced depending of the t -phase section (13, 15). It can be noticed that the corresponding three-dimensional refinements would require 34, 34, and 64 independent atoms, respectively. The refinement for the $P-3$ centrosymmetric space group ($t = 0 \text{ mod } (1/6k)$) leads to residual factors ($R = 0.058$) higher than the incommensurate option. The $P32$ and $P3$ three-dimensional space-groups give similar results ($R = 0.0470$ and $R = 0.0466$, respectively). From these results, it can be assumed that the structure is incommensurate since the residual factor is significantly lower ($R = 0.0406$).

DISCUSSION

Before discussing our experimental results, we briefly summarize the main concepts of the superspace formalism. As written above, four indices (h, k, l, m) are necessary to index each Bragg reflections. The main point of the superspace formalism is to consider that the satellites reflections

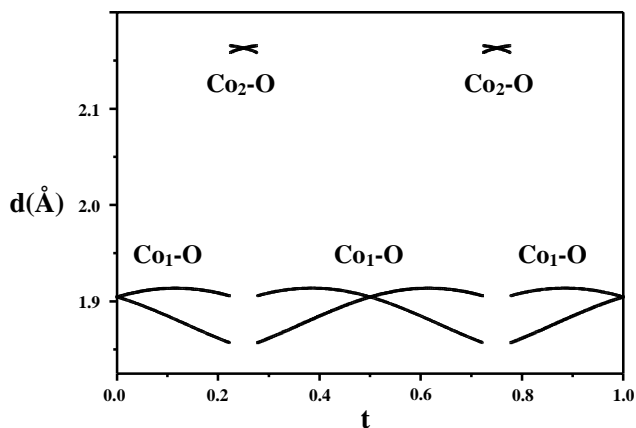


FIG. 4. Co-O distances versus t for $\text{Ba}_{1.1064}\text{CoO}_3$.

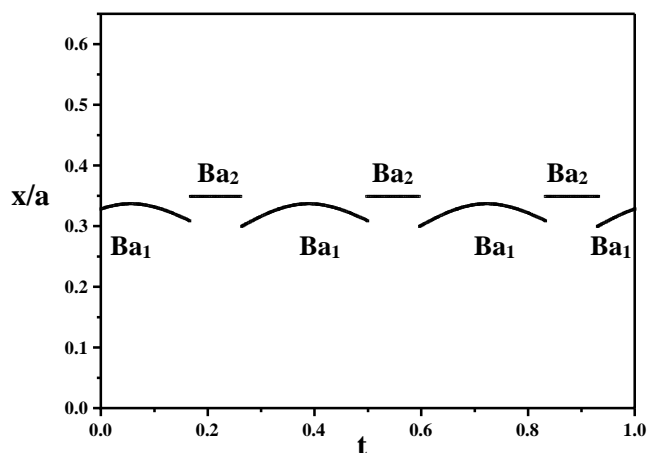


FIG. 5. Variation of the $x (= y)$ fractional coordinate of Ba1 and Ba2 versus the internal coordinate t .

are the orthogonal projection into three-dimensional space R_3 of lattice points of a four-dimensional reciprocal lattice defined in four-dimensional space R_4 (there is only one q vector). In this way, one can define a four-dimensional direct lattice in which the fourth dimension (x_4) is orthogonal to R_3 . In the R_4 space, the atoms lie on strings periodic along x_4 and defined by atomic modulation functions ($U(x_4)$). The real modulated structure can be depicted as a section orthogonal to x_4 of a four-dimensional periodic structure. For the commensurate case, the structure is defined for discrete sections, whereas the structure is defined in the whole domain of t ($t = x_4 - q.r_{av}$) for an incommensurate structure. Then, the atomic coordinates (x, y, z) are defined by the average atomic positions (x_0, y_0, z_0) plus the atomic modulation functions (AMF) ($U_x(x_4), U_y(x_4),$

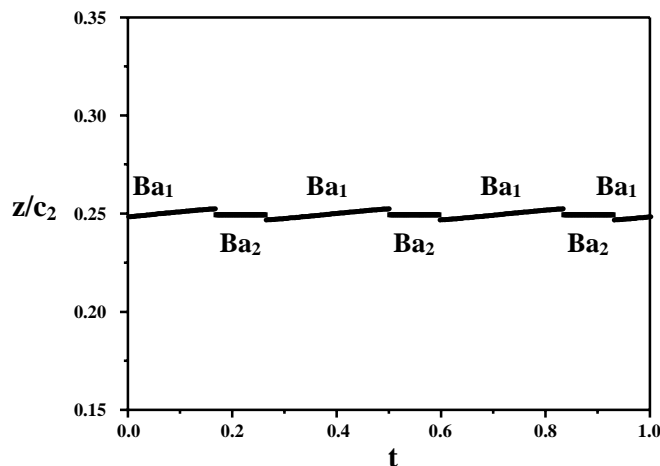


FIG. 6. Variation of the z fractional coordinate of Ba1 and Ba2 versus the internal coordinate t .

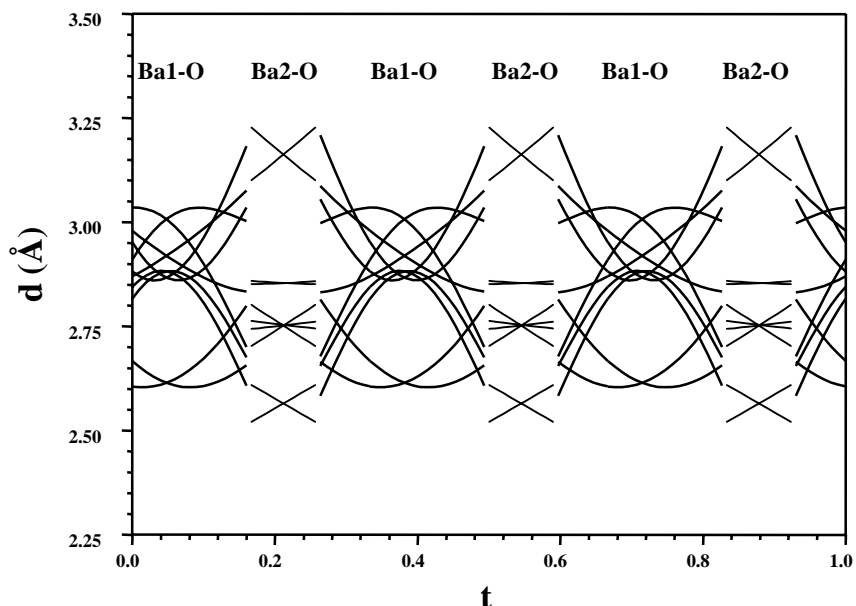


FIG. 7. Ba–O distances versus t for $\text{Ba}_{1.1064}\text{CoO}_3$.

$U_z(x_4)$). For more details on the superspace formalism see (28) and references therein.

Figure 1 represents the variation of the z component of the AMFs versus t for the $[\text{CoO}_3]$ subsystem. One can notice that the deviation from the ideal saw-tooth function is only noticeable at the limits of the domains especially for the oxygen atoms. As predicted by the model (15), the x and y modulation components of the oxygen are very small (Fig. 2). According to the superspace group, the symmetry forbids the modulation of the cobalt atom in the xy plane, as the average position is at the origin. The interatomic Co–Co and Co–O distances are plotted versus the internal coordinate t in Figs. 3 and 4.

The Co_1 – Co_1 distances between two adjacent face sharing octahedra are close to 2.4 \AA and shorter than the Co_1 – Co_2 distances between an octahedron and a trigonal prism ($\approx 2.8 \text{ \AA}$) (Fig. 4). The Co_1 –O distances range between 1.853 and 1.913 \AA for the octahedra and the Co_2 –O distances range between 2.169 and 2.178 \AA (Fig. 3). The Co_1 – Co_1 distances are in good agreement with the distance observed in the 2H-hexagonal perovskite BaCoO_3 (2.376 \AA) (29).

The cobalt atoms especially the Co_1 one (octahedral site) are slightly shifted from the center of the octahedron which is the consequence of the deviation of the displacive AMFs of the oxygen from the ideal saw-tooth function.

The variation of the x ($=y$) and z components for the [Ba] subsystem are given in Figs. 5 and 6. One can notice that the modulation components for Ba_1 (for Ba_2 , no modulation was introduced in the refinement) are very small. This point differs from the AMFs encountered for similar struc-

tures solved on the same basic model (16–18). The minimum Ba–O distances are, respectively, $d_{\min} = 2.599 \text{ \AA}$ for the Ba_1 site and $d_{\min} = 2.520 \text{ \AA}$ for the Ba_2 site. The variation of the Ba–O distances versus t is given in Fig. 7 with the upper limit of 3.25 \AA . Indeed, as the barium atoms and the oxygen atoms belong to the two different subsystems, there is no limit for the maximum distance.

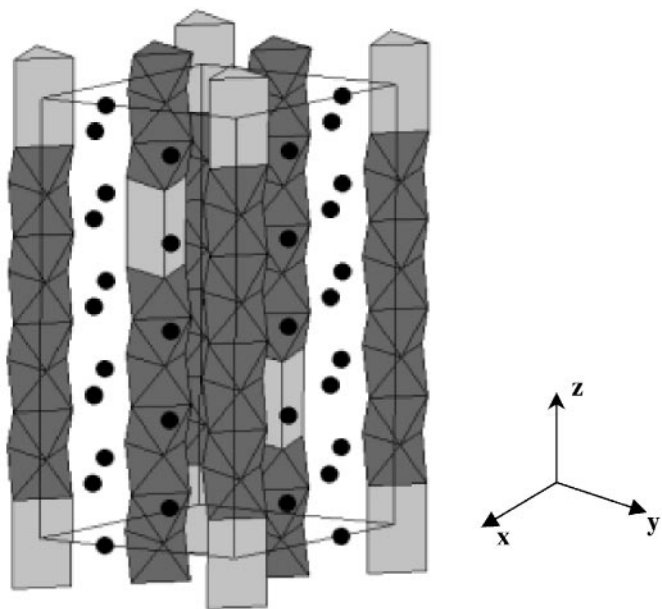


FIG. 8. Schematic representation of the $\text{Ba}_{10}\text{Co}_9\text{O}_{27}$ structure.

The composition of the studied single crystal ($x = 0.1064$) is close to the simplest composition $x = \frac{1}{9}$ (0.11111...), which corresponds to the superstructure $\text{Ba}_{10}\text{Co}_9\text{O}_{27}$ ($c_s \approx 5.c_2 \approx 9.c_1$). As developed in (15), the fractional value $x = p/k$ determines the sequence of octahedra and trigonal prisms along the chain. p is the number of trigonal prisms in the single sequential unit ($p = 1$), and ($k - p = 8$) corresponds to the number of octahedra. A schematic representation of the corresponding structure is given in Fig. 8. The space group of the superstructure is $P321$ as predicted (13–15). The sequence is 8 octahedra + 1 prism. For the experimental value $x = 0.1064$, it is straightforward to figure out that the previous sequence only suffers some ordered faults every few periods. A convenient way of giving the sequence of octahedra and trigonal prisms for any value of x is given by using the Farey tree (29) adapted to this case (15).

In our case, the value $x = 0.1064$ can be accurately approximated to $x \approx \frac{2}{19}$ (0.1053). Then the sequence is the juxtaposition of one (8 oct + 1 pr) (for $x = \frac{1}{9}$) plus one (9 oct + 1 pr) (for $x = \frac{1}{10}$). The sequence corresponds to a supercell $c_s \approx 30 c_1 \approx 75 \text{ \AA}$. One can figure out that the determination of this structure in the conventional crystallography will be tedious. All these results show clearly that the only strategy to accurately solve such structures is to use the superstructure formalism.

ACKNOWLEDGMENT

We thank V. Petricek for helpful comments and for adapting the JANA program to the model based on saw-tooth functions.

REFERENCES

1. J. Darriet and M. A. Subramanian, *J. Mater. Chem.* **5**, 543 (1995).
2. C. Dussarat, F. Grasset, and J. Darriet, *Eur. J. Solid State Inorg.* **32**, 557 (1995).
3. P. D. Battle, G. R. Blake, J. Darriet, J. G. Gore, and F. Weill, *J. Mater. Chem.* **7**, 1559 (1997).
4. M. Huvé, C. Renard, F. Abraham, G. V. Tendeloo, and S. Amelinckx, *J. Solid State Chem.* **135**, 1 (1998).
5. F. Grasset, F. Weill, and J. Darriet, *J. Solid State Chem.* **140**, 194 (1998).
6. P. D. Battle, G. R. Blake, J. Sloan, and J. F. Vente, *J. Solid State Chem.* **136**, 103 (1998).
7. G. R. Blake, J. Sloan, J. F. Vente, and P. D. Battle, *Chem. Mater.* **10**, 3536 (1998).
8. G. R. Blake, P. D. Battle, J. Sloan, J. F. Vente, J. Darriet, and F. Weill, *Chem. Mater.* **11**, 1551 (1999).
9. K. Boulahya, M. Parras, and J. M. Gonzalez-Calbet, *J. Solid State Chem.* **142**, 419 (1999).
10. K. Boulahya, M. Parras, and J. M. Gonzalez-Calbet, *J. Solid State Chem.* **145**, 116 (1999).
11. K. Boulahya, M. Parras, and J. M. Gonzalez-Calbet, *Chem. Mater.* **12**, 25 (2000).
12. K. Ukei, A. Yamamoto, Y. Watanabe, T. Shishidv, and T. Fukuda, *Acta Crystallogr. Sect. B* **49**, 67 (1993).
13. M. Evain, F. Boucher, O. Gourdon, V. Petricek, M. Dusek, and P. Bezducka, *Chem. Mater.* **10**, 3068 (1998).
14. O. Gourdon, V. Petricek, M. Dusek, P. Bezducka, S. Durovic, D. Gyepesova, and M. Evain, *Acta Crystallogr. Sect. B* **55**, 841 (1999).
15. J. M. Perez-Mato, M. Zakhour-Nakhl, F. Weill, and J. Darriet, *J. Mater. Chem.* **9**, 2795 (1999).
16. M. Zakhour-Nakhl, J. B. Claridge, J. Darriet, F. Weill, H. C. zur Loye, and J. M. Perez-Mato, *J. Am. Chem. Soc.* **122**, 1618 (2000).
17. M. Zakhour-Nakhl, F. Weill, J. Darriet, and J. M. Perez-Mato, *Int. J. Inorg. Mat.* **2**, 71 (2000).
18. M. Zakhour-Nakhl, J. Darriet, J. B. Claridge, H. C. Zur Loye, and J. M. Perez-Mato, *Int. J. Inorg. Mat.* **2**, 503 (2000).
19. S. Van Smaalen, *Phys. Rev. B* **43**, 11,330 (1991).
20. A. Janner and T. Janssen, *Acta Crystallogr. Sect. A* **36**, 399 (1980).
21. A. Janner and T. Janssen, *Acta Crystallogr. Sect. A* **36**, 408 (1980).
22. J. M. Perez-Mato, G. Madariaga, F. J. Zuniga, and A. Garcia Arribas, *Acta Crystallogr. Sect. A* **216** (1987).
23. S. Van Smaalen, *Crystallogr. Rev.* **4**, 79 (1995).
24. W. H. Henly, J. B. Claridge, P. L. Smallwood, and H. C. zur Loye, *J. Cryst. Growth* **204**, 122 (1999).
25. V. Petricek and M. Duseck, "Programs for Modulated and Composite Crystals." Institute of Physics, Praha, Czech Republic, 1998.
26. V. Petricek, A. Van der Lee, and M. Evain, *Acta Crystallogr. Sect. A* **51**, 529 (1995).
27. F. Boucher, M. Evain, and V. Petricek, *Acta Crystallogr. Sect. A* **52**, 100 (1996).
28. T. Janssen, A. Janner, A. Looijenga-Vos, and P. M. de Wolff, "International Tables for Crystallography," Vol. C, p. 797. Kluwer Academic, Dordrecht, 1996.
29. H. Taguchi, Y. Takeda, F. Kanamaru, M. Shimada, and M. Koizumi, *Acta Crystallogr. Sect. B* **33**, 1299 (1977).
30. "Royal Society Mathematical Tables," Vol I. Royal Society, Cambridge University Press, Cambridge 1950. [The Farey series of order 1025]